

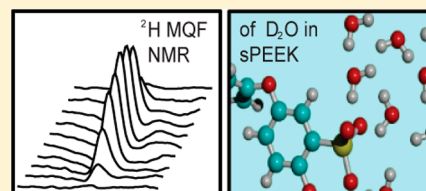
Investigating the Water in Hydrated sPEEK Membranes Using Multiple Quantum Filtered  $^2\text{H}$  NMR Spectroscopy

Joel M. Woudstra and Kristopher J. Ooms\*

Department of Chemistry, The King's University College, 9125-50 St. Edmonton, Alberta, Canada T6B 2H3

## Supporting Information

**ABSTRACT:** Double and zero quantum filtered  $^2\text{H}$  NMR spectroscopy is used to study the structure and dynamics of  $\text{D}_2\text{O}$  in sulfonated poly(ether ether ketone) membranes as a function of membrane hydration. Both residual quadrupolar coupling constants and  $T_2$  relaxation values are obtained as a function of hydration. The residual couplings vary from 160 Hz at low hydration to 30 Hz at high hydration. The  $T_2$  relaxation times range from 3 to 14 ms, with the high hydration values having longer  $T_2$ . Results from this study are compared to results obtained for Nafion membranes, revealing similarities and differences in the water environments of the two membranes that result from the structure of the polymers and can be related to properties such as water diffusion.



## INTRODUCTION

The development of cost-effective, clean energy technologies is a key requirement for reducing the world's reliance on fossil fuels.<sup>1</sup> The optimal way to harness the chemical energy in low carbon fuels like  $\text{H}_2$  and  $\text{CH}_3\text{OH}$  is to use a highly efficient fuel cell. A key component of many commercial fuel cells is a polymer electrolyte membrane (PEM) used to separate the anode and cathode. The efficiency of a PEM fuel cell is affected by the membrane's ability to conduct ions.<sup>2</sup> Even after decades of research, Nafion remains the standard polymer membrane for commercially available PEM fuel cells; however, drawbacks such as high production cost, methanol permeability, and limited operational temperature ranges have led to interest in other membranes such as sulfonated poly(ether ether ketone) (sPEEK).<sup>3–10</sup>

In sulfonated polymer membranes such as sPEEK and Nafion, the ionic conductivity depends on the structure and dynamics of water in the hydrated membrane.<sup>11</sup> The models used to describe membrane hydration typically have two types of water molecules. The molecules that spend significant time in the first hydration sphere of the sulfonate experience anisotropic motion and are often referred to as bound waters. Water molecules that form the channel systems in the membrane are referred to as the bulk water.<sup>12–15</sup> Based on experiment as well as molecular dynamics (MD) simulations, there are up to 6 or 7 waters in the first hydration sphere of the sulfonate depending on the hydration level of the membrane.<sup>3,5,6,15–18</sup> A quasielastic neutron scattering study of Nafion suggests that these bound waters have mean jump times between 0.2 and 0.7 ns, and the more mobile bulk waters have jump times between 2.5 and 9 ps.<sup>16</sup>

The molecular structure of sPEEK consists of an aromatic backbone that is directly sulfonated when PEEK is treated with sulfuric acid as shown in Figure 1a.<sup>19</sup> In contrast, Nafion, has a fluorinated aliphatic backbone with sulfonates attached to side chains, Figure 1b. The sPEEK polymer chains are less flexible

Figure 1. Chemical structures of (a) sPEEK and (b) Nafion.

than those of Nafion. A consequence of this decreased flexibility is that the sulfonates are further apart in sPEEK.<sup>3</sup> Current models also suggest that the channel structure in sPEEK is more branched and narrower than in Nafion.<sup>4,20</sup> The conductivity and water diffusion in Nafion is faster than in sPEEK likely due to the differences in the channel structure.<sup>15</sup> As hydration models are being refined, particularly using MD simulations, there is a need for a wider range of molecular level experimental techniques that can probe the local structure and dynamics of water in these hydrated membranes.

Multiple quantum filtered (MQF)  $^2\text{H}$  NMR spectroscopy is a useful way of exploring the molecular level structure and dynamics of water in hydrated systems.<sup>21–29</sup> By analyzing  $^2\text{H}$  MQF spectra, small residual quadrupolar couplings,  $C_Q^{\text{res}}$ , and  $T_2$  relaxation times can be determined. The residual quadrupolar couplings arise when the water molecules do not experience isotropic motion but are restricted through interactions with a large molecule or solid matrix. These couplings can act as a probe for changes in local structure or the equilibrium between

Received: October 9, 2012

Revised: November 20, 2012

Published: December 7, 2012

water in distinct environments. For example, at low hydrations  $^2\text{H}$  quadrupolar couplings of water in ionomers have been measured for tightly bound waters as an indicator of average channel alignment under different polymer preparation methods.<sup>30–34</sup> However, it is not always easy to accurately measure quadrupolar splittings in NMR spectra acquired with common pulse sequences (single-pulse or Hahn-echo experiments), particularly when the couplings become small. The relaxation rates obtained from the MQF experiments are related to water motion and provide a sensitive method of measuring changes in water dynamics under different conditions. An advantage to using MQF spectroscopy is that different sites with  $C_Q^{\text{res}}$  and  $T_2$  can often be observed and multiple water environments can be explored from a structural and dynamic perspective.

In this work,  $^2\text{H}$  MQF NMR spectroscopy of  $\text{D}_2\text{O}$  in sPEEK membranes at various hydration levels is used to probe the molecular level structure and dynamics of water and then compared to results previously obtained using Nafion.<sup>27</sup>

## EXPERIMENTAL SECTION

**Membrane Treatment.** Strips of sPEEK (fumapem E-750, Fumatech, DS = 45%, 50  $\mu\text{m}$  thickness) between 9 and 24  $\text{cm}^2$  were treated as follows to clean and fully protonate the membranes. The membranes were heated ( $\sim 70^\circ\text{C}$ ) in a 3%  $\text{H}_2\text{O}_2$  (Fisher) solution for 10 min, washed in boiling distilled water for 30 min, heated in a 3 mol/L  $\text{H}_2\text{SO}_4$  solution for 1 h, and then washed in boiling distilled water for another 30 min. The sPEEK strips were dehydrated under vacuum until the weight stabilized. Previous studies indicate that dried sPEEK has around 1.5 waters that can not be readily removed under vacuum.<sup>14</sup> This treatment procedure is expected to raise the degree of sulfonation (DS) only slightly.<sup>19</sup> The anhydrous membranes were rehydrated with  $\text{D}_2\text{O}$  (Cambridge Isotope Laboratories, 99.9% D) by soaking the membranes in  $\text{D}_2\text{O}$ , and excess water was wiped off the surface before weighing. Membranes were soaked for between 3 and 48 h. Hydration values,  $\lambda$ , in units of  $\text{D}_2\text{O}$  per sulfonate, were calculated based on the mass of  $\text{D}_2\text{O}$  absorbed by the membrane. These masses were measured and recorded immediately before and after performing the NMR experiments. The trends in hydration were also monitored by comparing the  $^2\text{H}$  NMR signal intensities from a single-pulse experiment; a linear correlation between the signal intensities and  $\lambda$  values confirmed the hydration levels.

**Data Acquisition.** Each sample was placed in a 5 mm solution NMR tube by first coiling it into a Teflon tube liner and then sliding it into the NMR tube. The NMR tube and Teflon tube liner were sealed with Parafilm for NMR experiments. The effects of sample placement were assessed by monitoring the proton and deuterium NMR line shapes and widths in an attempt to reduce the effects of magnetic susceptibility differences between the experiments. All NMR spectra were collected on a high resolution Bruker Avance 400 MHz NMR spectrometer at The King's Center for Molecular Structure using a Bruker ATMA multinuclear probe tuned at 61.42 MHz for  $^2\text{H}$  with a  $180^\circ$  pulse optimized to 19.6  $\mu\text{s}$ . Experiments were referenced to liquid  $\text{D}_2\text{O}$  set at 0 Hz.  $T_1$  relaxation values were obtained using a standard inversion recovery pulse sequence and analyzed using the Bruker software. Double and zero quantum filtered (DQF and ZQF) experiments were carried out using the MQF pulse sequence shown in Figure 2.<sup>23</sup> Between 128 and 512 transients were

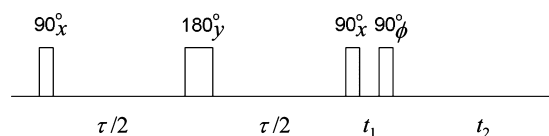


**Figure 2.** MQF pulse sequence used. The sequence consists of a  $90^\circ$  excitation pulse, an evolution time,  $\tau$ , and a pair of  $90^\circ$  filter pulses. A  $180^\circ$  refocusing pulse is placed in the middle of the evolution time to remove the effect of chemical shift and field inhomogeneities during  $\tau$ . The phase cycling is used to select either double or zero quantum coherences. The four-step phase cycle for the last pulse is  $x, y, -x, -y$  for both ZQF and DQF. The detection phase cycles for ZQF and DQF are  $x, y, -x, -y$ , and  $x, -y, -x, y$ , respectively. The delay  $t_1$  was set to 10  $\mu\text{s}$  and  $t_2$  was 1 s allowing for full relaxation of the NMR signal ( $T_1 < 100$  ms).

summed in order to achieve a signal-to-noise ratio greater than 20 at  $\tau_{\text{max}}$  in the DQF spectra; a 1 s recycle delay was used between transients. The evolution time,  $\tau$ , was varied from 0.2 to 140 ms and 22 ZQF and 22 DQF spectra were acquired for each hydration level of which 10 ZQF and 10 DQF spectra were selected that best represented the full range of  $\tau$  values for which signal build up and decay was observed. The spectral fitting was performed using Matlab and employed a multi-variable, nonlinear, least-squares regression method to minimize the residual between the calculated and experimental spectra. ZQF and DQF spectra were fit simultaneously during the fitting procedure to ensure the quantitative inclusion of all of the water environments. Due to the low intensity of the DQF spectra, the data fitting was performed by weighting the residual for the DQF spectra ten times greater than that of the ZQF. This resulted in better fits of the DQF spectra without significantly affecting the ZQF fits.

The primary source of error in the data is experimental. Five different pieces of membrane were fully analyzed and two additional pieces were used to check for reproducibility at specific hydrations (see Table S1 in the Supporting Information). The analysis of the data confirms variation in the parameters obtained from different samples of similar hydrations. Some of this error may be from sample alignment and field inhomogeneities during the NMR experiments, but the largest source of error likely results from sample preparation; all samples in this study were treated as described above. A detailed study on the effects of sample preparation of sPEEK may be conducted in the future. The variations in parameters arising from these experimental sources of error do not affect the interpretation of the results or the comparison to the results obtained from Nafion.

## RESULTS AND DISCUSSION

Double and zero quantum filtered  $^2\text{H}$  NMR spectra were acquired from samples of sPEEK with varying levels of hydration. Figure 3 shows representative ZQF and DQF spectra from a membrane at low hydration (a and b) and high hydration (c and d), acquired as a function of evolution time,  $\tau$ . The presence of signal in the DQF experiments indicates that at both hydration levels  $^2\text{H}$  nuclei on water molecules are experiencing a residual quadrupolar coupling due to water interacting with the polymer. The signal from the DQF experiment was low compared to the signal in the first ZQF experiment (the first ZQF spectrum at each hydration level was used to normalize the DQF intensities from different samples). At the lowest hydration level, the maximum normalized DQF

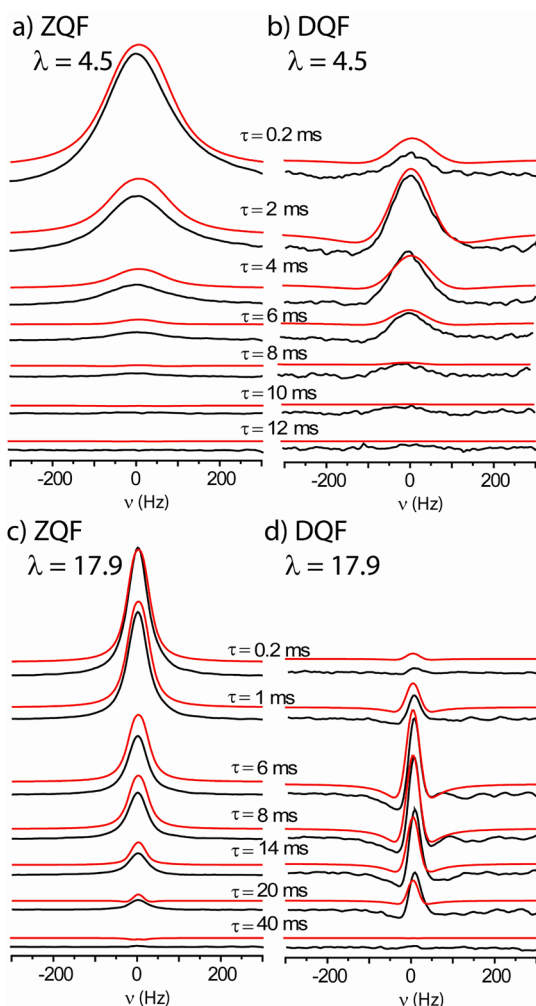


**Figure 3.** Example  $^2\text{H}$  ZQF and DQF spectra of  $\text{D}_2\text{O}$  in sPEEK as a function of  $\tau$  for  $\lambda = 4.5$   $\text{D}_2\text{O}$ /sulfonate, (a and b) and  $\lambda = 17.9$   $\text{D}_2\text{O}$ /sulfonate (c and d). The red lines are the spectral fits obtained using eqs 1 and 2 and simultaneously fitting 10 ZQF and 10 DQF spectra.

signal intensity compared to the first ZQF peak was 0.035 and decreased to 0.015 at the highest hydrations (Figure 4a). For comparison, the normalized signal intensity was around 0.14 for spinal disc tissue<sup>28</sup> and 0.6 for low hydration Nafion.<sup>27</sup> Although the low DQF signal intensity observed for sPEEK could arise because only a small fraction of the water experiences the anisotropic motion, it is more likely that it is caused by an interplay between  $C_Q^{\text{res}}$  and  $T_2$ . In most cases, the DQF signal build-up rate is determined by  $C_Q^{\text{res}}$  (large  $C_Q^{\text{res}}$  leads to rapid signal build-up) and the signal decay is determined by  $T_2$ . If  $T_2$  is rapid compared to the time required to build up the DQF signal, low signal intensity will be observed. Previous studies have indicated that the parameter  $\tau_{\text{max}}$ , the time at which maximum DQF signal intensity is observed, can be useful for capturing the combined effects of  $C_Q^{\text{res}}$  and  $T_2$ . Figure 4b shows a plot of  $\tau_{\text{max}}$  for the sPEEK membranes as a function of hydration (black squares). The  $\tau_{\text{max}}$  values are all between 1 and 10 ms and increase with increasing hydration. This range of  $\tau_{\text{max}}$  values is small when compared to the  $\tau_{\text{max}}$  values for Nafion membranes which ranged from 3 to 33 ms (Figure 4b, red points).<sup>27</sup> This clearly indicates significant differences between the water in sPEEK and Nafion and that the lower DQF signal

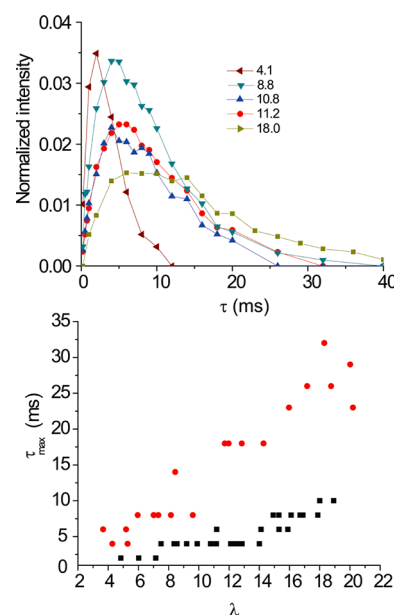


**Figure 4.** (a) Plot of the DQF signal intensity as a function of  $\tau$ . The signal is normalized to the intensity of the first ZQF spectrum for each hydration level. (b) A plot of the  $\tau$  at which maximum DQF signal intensity is observed versus the level of hydration,  $\lambda$ , for sPEEK (black squares) and Nafion (red circles).<sup>27</sup>

intensity observed in sPEEK arises primarily from an interplay between  $C_Q^{\text{res}}$  and  $T_2$ .

To obtain values for  $C_Q^{\text{res}}$  and  $T_2$  the DQF and ZQF spectra were fit to analytical equations<sup>35</sup>

$$S_{\text{DQF}}(\tau, \omega_2) = \sin(Q\tau) \exp(-\tau/T_2) \left[ \frac{\omega_2 - \delta_0 + Q}{(\omega_2 - \delta_0 + Q)^2 + (1/T_2^*)^2} - \frac{\omega_2 - \delta_0 - Q}{(\omega_2 - \delta_0 - Q)^2 + (1/T_2^*)^2} \right] \quad (1)$$

$$S_{\text{ZQF}}(\tau, \omega_2) = \cos(Q\tau) \exp(-\tau/T_2) \left[ \frac{1/T_2^*}{(\omega_2 - \delta_0 + Q)^2 + (1/T_2^*)^2} + \frac{1/T_2^*}{(\omega_2 - \delta_0 - Q)^2 + (1/T_2^*)^2} \right] \quad (2)$$

that depend on the experimental evolution time,  $\tau$ , the  $T_2$  relaxation time, and the quadrupolar half splitting  $Q$ .  $\omega_2$  is the frequency of the spectrum and  $\delta_0$  is the frequency offset of the peak in  $\text{s}^{-1}$ .  $T_2^*$  is related to  $T_2$  by  $1/T_2^* = \pi W + 1/T_2$  where  $W$  is a line broadening factor resulting from inhomogeneous broadening.  $Q$  is related to the  $C_Q^{\text{res}}$  by

$$Q(\theta, \phi) = \frac{3\pi}{4} C_Q^{\text{res}} [3\cos^2\theta - 1 - \eta\sin^2\theta \cos 2\phi] \quad (3)$$

where  $\eta_Q$  is the asymmetry parameter of the electric field gradient and the angles  $\theta$  and  $\phi$  define the orientation of the EFG in the magnetic field (in our simulations  $\eta_Q$  was assumed to be 0). The simulated spectra were obtained by unbiased averaging of  $\theta$  dependent lineshapes that sampled the range of

$\theta$  values ( $0$ – $360^\circ$ ). Example fits are shown in Figure 3 (red lines).

Equations 1 and 2 can be broken into two parts. The first part of each equation describes the evolution of the NMR signal during the evolution time  $\tau$  and dictates the signal intensity as a function of  $\tau$ . The second part of each equation, in the square brackets, arises from the evolution of the signal during the acquisition time and leads to the line shape observed.

When fitting DQF and ZQF spectra, the motion of the water can affect how the data is analyzed. If the water molecules have very short characteristic correlation times compared to the NMR Larmor frequency,  $\omega_0$ , the motion is said to be in the extreme narrowing regime,  $\omega_0\tau_c \ll 1$ . In this case, the  $T_2$  relaxation rate of the zero quantum signal is  $3/5$  that of the double quantum signal.<sup>27</sup> Previous research has indicated that, for Nafion, the important water motion is in the extreme narrowing regime and the  $3/5$  factor was required to fit the data. The same is true for sPEEK, where inclusion of the  $3/5$  factor resulted in better fits of the DQF and ZQF spectra. This indicates that the characteristic correlation time for the motion that dominates the  $T_2$  relaxation is much shorter than  $10^{-8}$  s, consistent with conclusions from MD simulations and  $^1\text{H}$  NMR experiments.<sup>3,14</sup>

A second observation resulting from the fitting procedure is that all the spectra could be fit using a single site, i.e., one set of  $C_Q^{\text{res}}$  and  $T_2$  values; addition of a second site did not significantly improve the fits. This is different than Nafion, where two different water sites were needed at elevated hydrations, corresponding to water that had a  $C_Q^{\text{res}}$  between 20 and 50 Hz and water that had  $C_Q^{\text{res}}$  values  $<10$  Hz.<sup>27</sup> The negligible  $C_Q^{\text{res}}$  water sites in Nafion were postulated to arise from water molecules in the core of the bulk water channels. These core waters are highly mobile and spend very little time interacting with the sulfonate groups during the NMR experiment. The lack of such a site in sPEEK indicates that the water domains in sPEEK are not as large as those in Nafion. This provides more experimental evidence for the smaller water environments in sPEEK (less phase-segregated), complementing small-angle X-ray scattering and MD studies.<sup>3,4</sup>

**Analysis of the Quadrupolar Coupling Data.** The values obtained for  $C_Q^{\text{res}}$  at various hydrations are represented in Figure 5a (black squares); Table S1 in the Supporting Information contains a list of all of the parameters obtained. The  $C_Q^{\text{res}}$  values for  $\text{D}_2\text{O}$  in sPEEK decrease as hydration increases, from 160 Hz at  $\lambda \approx 5$  to 30 Hz above  $\lambda \approx 11$ . Figure 5a also contains the values obtained from water in Nafion for comparison (red circles and blue triangles). The values obtained at the lowest hydration are consistent with quadrupolar splittings observed using single pulse experiments at low hydration for  $\text{D}_2\text{O}$  in extruded Nafion and other ionomers.<sup>30,32,34</sup>

The decreasing  $C_Q^{\text{res}}$  with increasing hydration is typical of hydrated materials and arises because as hydration increases, each water molecule spends less time in sites that lead to anisotropic motion. In a simple two domain model the resulting average quadrupolar coupling, will be a population weighted average of water in the bound and bulk domains

$$C_Q^{\text{res}} = f_b \langle C_Q^k \rangle_b \quad (4)$$

where  $f_b$  is the combined fraction of waters in all the binding sites and  $\langle C_Q^k \rangle_b$  is the averaged quadrupolar coupling experienced by the  $^2\text{H}$  of  $\text{D}_2\text{O}$  in the bound sites. In our

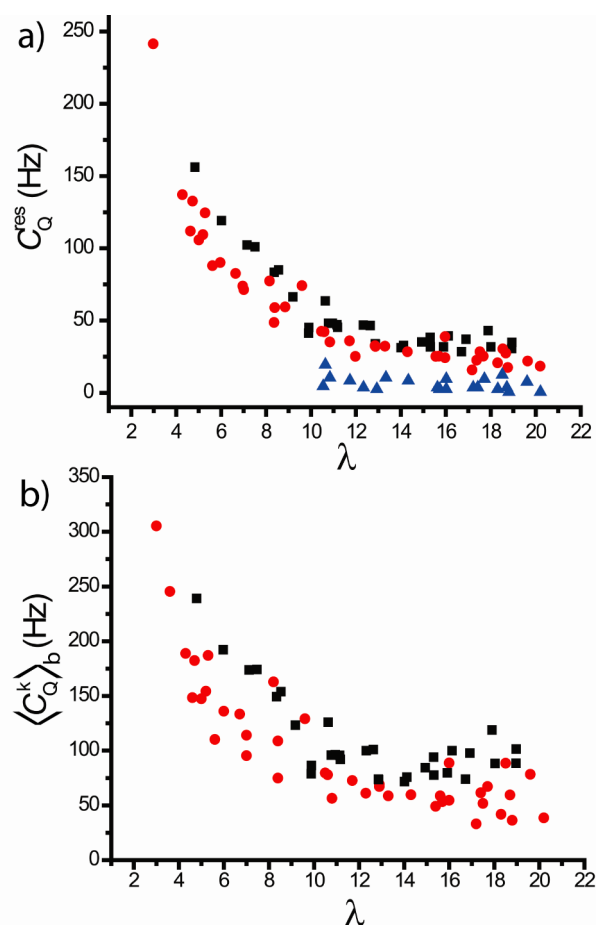


**Figure 5.** (a) Plot of the residual quadrupolar coupling constants as a function of hydration. (b) Plot of  $\langle C_Q^k \rangle_b$  values as a function of hydration. The black squares are for water in sPEEK, and the red circles and blue triangles are data obtained for the water sites in Nafion (only the red data points were used in panel b).<sup>27</sup>

analysis we assume the water experiences a significant quadrupolar coupling only when it is bound to the sulfonate. When the water is in the bulk the coupling is expected to be almost completely averaged by the rapid motion, resulting in a coupling too small to detect. In the study of Nafion, this model provides the basis for assigning the negligible  $C_Q^{\text{res}}$  sites in Nafion to water at the center of the phase-segregated water environments where they do not interact with the sulfonates enough to build up a significant coupling.

It is remarkable that the  $C_Q^{\text{res}}$  values observed for water in sPEEK are so similar to those observed for Nafion at the same hydration levels. MD simulations of Nafion and sPEEK provide the number of water molecules in the first coordination sphere of the sulfonate as a function of hydration; coordination numbers (CN) for all  $\lambda$  values were obtained by interpolating between the available data.<sup>3,6,36</sup> The CN values can be used to determine the fraction of waters bound to the sulfonates,  $f_b$ , and then calculate the quadrupolar coupling in the bound sites,  $\langle C_Q^k \rangle_b$ . Figure 5b shows a plot of the  $\langle C_Q^k \rangle_b$  versus  $\lambda$ . The quadrupolar coupling in the bound site changes dramatically below  $\lambda = 10$  where MD studies indicate the CN also rapidly changes. Like the  $C_Q^{\text{res}}$  values, the  $\langle C_Q^k \rangle_b$  values of sPEEK are not significantly different from those of Nafion. This suggests that, at the hydration levels studied, the  $\langle C_Q^k \rangle_b$  values are not sensitive to structural differences, such as polymer flexibility and



sulfonate-sulfonate separation.<sup>3,17,36</sup> Instead  $\langle C_Q^k \rangle_b$  is dominated by the intermolecular interactions within the first coordination sphere of the sulfonate. While further studies of other sulfonated membranes are required, these preliminary results suggest that  $\langle C_Q^k \rangle_b$  is a useful local probe of the first coordination sphere around the sulfonate, even for structurally different polymers.

In a previous  $^1\text{H}$  NMR study, DQF spectra of  $\text{H}_2\text{O}/\text{H}_3\text{O}^+$  revealed that a signal could be detected for Nafion but not for sPEEK when the membranes were dehydrated ( $\lambda \approx 1.5$ ).<sup>14</sup> When the  $\lambda$  was increased to 2.6, a small DQF peak from the sPEEK was observed at  $\tau = 0.32$  ms which disappeared as the hydration was increased due to very small residual dipolar couplings. Comparable observations are made in the  $^2\text{H}$  DQF studies of Nafion and sPEEK at the lowest hydrations. For Nafion at  $\lambda = 3$ ,  $^2\text{H}$  DQF spectra were obtained and could be fit, whereas for sPEEK at  $\lambda = 3$ , the DQF peak was so small that useful fits could not be obtained; the normalized DQF peak intensity was less than 1% of the first ZQF spectrum and appeared at  $\tau$  values below 1 ms with a  $\tau_{\text{max}}$  close to 0.5 ms. Without being able to fit the data it is difficult to determine if the low signal intensity for sPEEK at  $\lambda = 3$  arises because of a very small coupling or very rapid  $T_2$  relaxation, but given the small  $T_2$  values observed at higher hydrations, it is reasonable that short  $T_2$  values are a major contributor. The ability to measure DQF signal in this study indicates that the quadrupolar interaction of  $\text{D}_2\text{O}$  is a more sensitive probe than the dipolar interaction of  $\text{H}_2\text{O}$  at higher membrane hydrations.

**Analysis of Relaxation Times.** Figure 6a,b shows the  $^2\text{H}$  longitudinal and transverse relaxation rates,  $1/T_1$  and  $1/T_2$ , respectively, for  $\text{D}_2\text{O}$  in sPEEK at various hydration levels (black squares), as well as the data previously measured for Nafion (red circles).<sup>27</sup> It is clear that the  $1/T_2$  and  $1/T_1$  values are much greater in sPEEK. The relaxation rates for  $\text{D}_2\text{O}$  interacting with a surface in the extreme-narrowing regime can be described as a population weighted average of the relaxation rates in the different domains.<sup>37</sup> According to relaxation theory, the relaxation rate in each site will be proportional to the characteristic correlation time,  $\tau_c$ , and the square of the effective quadrupolar coupling experienced by the  $^2\text{H}$  in the site.<sup>38</sup> The observation that the relaxation rates are much faster in sPEEK than in Nafion while the quadrupolar parameters are similar indicates that the water molecules in the two membranes have different dynamics. Since rates are proportional to  $\tau_c$ , the slowest motions (large  $\tau_c$ ) in the extreme narrowing regime will contribute the most to the enhanced relaxation rate. It is expected that the motion of water in the bulk phase will be fast and not be the dominant contributor to the enhanced relaxation rates. Since  $\langle C_Q^k \rangle_b$  is the motionally averaged quadrupolar coupling of the deuterium when the  $\text{D}_2\text{O}$  is bound to the sulfonate, the fact that  $\langle C_Q^k \rangle_b$  is nearly the same for Nafion and sPEEK indicates that the motion of the water molecule in the bound site is also similar. The different relaxation rates are therefore caused by differences in the exchange correlation time of water between the bound and bulk environments. The observation of larger exchange correlation times in sPEEK compared to Nafion is consistent with the proton exchange activation energies determined at low hydration using  $^1\text{H}$  NMR.<sup>14</sup>

Since the structure of the bound water is similar in the two materials, the cause of the dramatically different exchange correlation times must be due to the structure and energy of the transition state. MD simulations have suggested that the

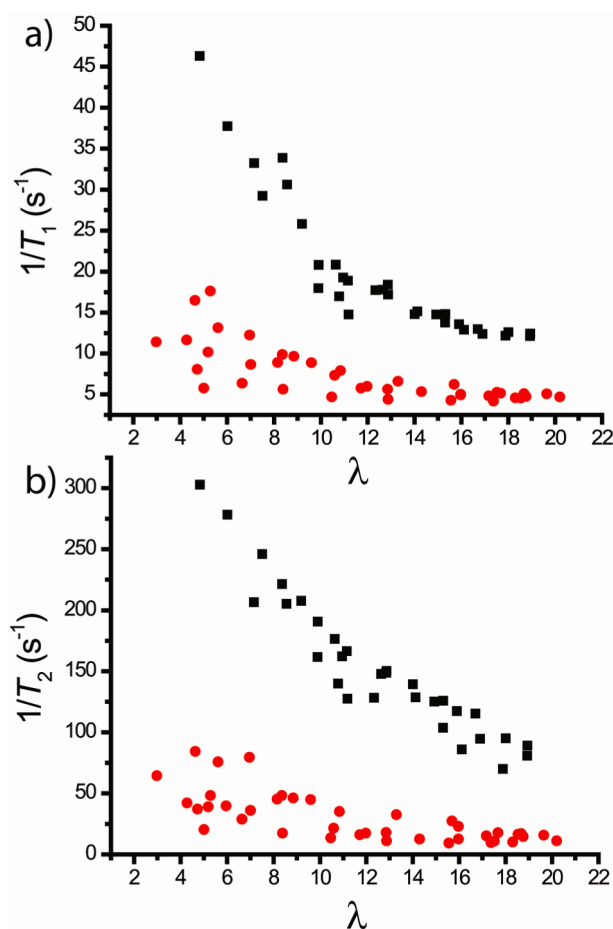


**Figure 6.** Plots of the relaxation rates as a function of hydration: (a)  $1/T_1$  and (b)  $1/T_2$ . The black squares are for water in sPEEK, and the red circles are those obtained previously for water in Nafion.<sup>27</sup> Values for  $T_2$  relaxation are based on the DQF signal and are 5/3 longer than those from the ZQF signal (see text).

hydrogen bond network within the bulk water regions is more structured in Nafion than in sPEEK likely due to the larger nanophase segregation.<sup>3,6</sup> As a water molecule exchanges from the bound to the bulk environment the energy of the transition state will be decreased by the availability of hydrogen bonds. It is likely that the more structured hydrogen bond network in the bulk phase of Nafion also leads to the availability of more and/or stronger hydrogen bonds in the transition state, lowering the activation energy and exchange correlation time. Although studies of other polyaromatic membranes are required, it may be that  $T_2$  can be used as an indirect probe of the structure of the hydrogen bond network and, by extension, the nanophase segregation in sPEEK. Such an experimental probe could be useful for researchers preparing other polyaromatic membranes with increased nanophase segregation to more closely approximate the behavior of water in Nafion.

The water self-diffusion coefficient,  $D_{\text{H}_2\text{O}}$ , is an important macroscopic parameter used to quantify membrane performance.  $D_{\text{H}_2\text{O}}$ 's for sPEEK and Nafion are almost the same at high water content, but as hydration drops, the diffusion of water decreases faster in sPEEK than in Nafion.<sup>15</sup> The lower rate of diffusion in sPEEK is one of the reasons for the poorer performance of sPEEK-based PEM fuel cells. Studies of the diffusion constant in Nafion and different copolymers of Nafion

suggest that the single phase polymer membranes do not show significant anisotropy in the  $D_{\text{H}_2\text{O}}$  parallel and perpendicular to the membrane surface.<sup>31</sup>

The diffusion constants reported represent the apparent diffusion of water and are affected by two microscopic motions, the diffusion of water through the bulk and the amount of time a water spends "bound" to the sulfonate sites.<sup>4</sup> This molecular level model of motion suggests that the time a water spends bound to the sulfonate, the exchange correlation time  $\tau_c$  will impact the overall diffusion coefficient. The extent to which  $\tau_c$  impacts  $D_{\text{H}_2\text{O}}$  will depend on the overall structure of the water environments including the nanophase segregation and the number of waters in the bulk and bound sites.<sup>5</sup> If the exchange time is an important part of the overall water diffusion, a correlation between the  $T_2$  values and the water diffusion constants should be observed as both will be proportional to  $1/\tau_c$ . The extent to which the exchange rate influences  $D_{\text{H}_2\text{O}}$  will be indicated by the slope of the correlation line, with a steeper slope indicating the  $D_{\text{H}_2\text{O}}$  is more sensitive to changes in the rate of exchange.

Figure 7a shows the plot for sPEEK; the diffusion constants at various hydration levels were calculated from a best fit line

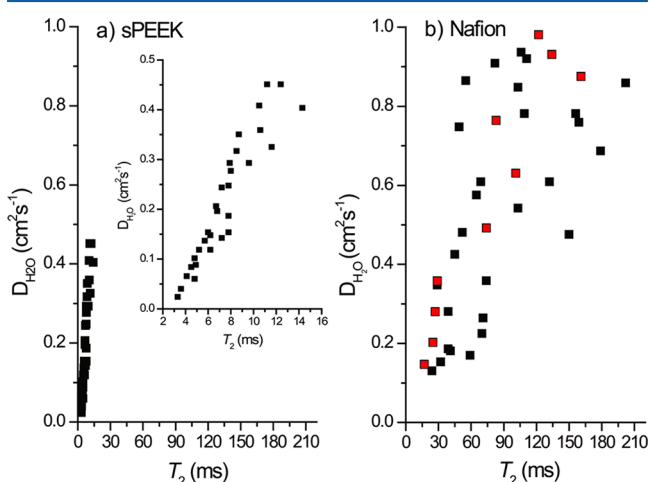


**Figure 7.** Plots of the water diffusion coefficient versus  $T_2$  for (a) sPEEK and (b) Nafion.<sup>27</sup>  $D_{\text{H}_2\text{O}}$  was calculated based on the data of Kreuer.<sup>4</sup> The red points are the points from a single membrane piece in the Nafion study and show that, despite the scatter due to sample preparation, the general trend of increasing  $D_{\text{H}_2\text{O}}$  with increasing  $T_2$  holds.

through the diffusion data of Kreuer.<sup>4</sup> It is clear from Figure 7a that a correlation between  $T_2$  and  $D_{\text{H}_2\text{O}}$  does exist. Figure 7b shows that the correlation is much weaker in Nafion due to the greater scatter in  $T_2$  data arising from variations in sample preparation; the red dots in Figure 7b are the data for a single membrane piece and show that, despite the scatter, larger  $T_2$  values do correspond to larger diffusion constants. The slopes of the two correlations are different, with sPEEK having a much larger change in  $D_{\text{H}_2\text{O}}$  over a narrower range of  $T_2$  values. This suggests that the exchange process between water bound to the sulfonates and the bulk has a stronger effect on the overall diffusion of water in sPEEK than in Nafion, likely because of the lower nanophase segregation in sPEEK.

## CONCLUSIONS

$^2\text{H}$  MQF NMR spectroscopy has been used to obtain quadrupolar coupling and NMR relaxation parameters of water in sPEEK as a function of hydration. These results, when compared to those obtained with Nafion, allow for a model of water in Nafion and sPEEK to be developed that connects the polymer structures and properties to molecular level structure and dynamics of water. Four general conclusions can be drawn:

1. These experiments support the idea that two general water domains exist in the membranes: waters that are closely associated with the sulfonates and waters that are in a bulk water environment within the membrane. The results indicate that the hydrated sulfonate sites provide a restricted environment where the  $^2\text{H}$  in the  $\text{D}_2\text{O}$  experiences a quadrupolar coupling that depends on the local structure in the first coordination sphere of the sulfonate, particularly the water coordination number and not on the structure of the polymer backbone.

2. There are observable differences in the bulk domains of the two membranes. The sPEEK membranes show a single type of water which exchanges between the sulfonate coordination sphere and the bulk water, whereas Nafion shows evidence of an additional type of water molecule that spends very little time interacting with the sulfonates and has a negligible  $C_Q^{\text{res}}$  value.

3. Water rapidly exchanges between the bound sites and the bulk water phase resulting in small  $C_Q^{\text{res}}$  values that depend on the number of water molecules coordinated to the sulfonates. The exchange correlation times between the bound and bulk water are larger in sPEEK (exchange is slower), possibly due to the less well developed internal structure of the bulk water environment which is caused by the lower nanophase segregation resulting from the greater rigidity of the sPEEK polymer.

4. The presence of a correlation between  $T_2$  and the water diffusion coefficient in sPEEK indicates that the exchange dynamics between the bound and bulk phase is an important component of the water diffusion through the membrane. The slope of the correlation line suggests exchange plays a more important role in diffusion of water in sPEEK than in Nafion. This provides a possible molecular level explanation for the differences in conductivity in the two materials and their resulting performance in PEM fuel cells.

Although these findings will have to be tested against other sulfonated membranes, this initial comparison between two well studied membranes shows the potential of using  $^2\text{H}$  MQF NMR to provide useful information about hydrated polymer membranes. The sensitivity of  $C_Q^{\text{res}}$  and  $T_2$  to structure and dynamics will prove useful for monitoring the molecular level changes in structure that occur due to membrane preparation, degradation, and variation in temperature.

## ASSOCIATED CONTENT

### Supporting Information

$C_Q^{\text{res}}$  and  $T_2$  values obtained from the fitting of the DQF and ZQF spectra. This material is available free of charge via the Internet at <http://pubs.acs.org>.

## AUTHOR INFORMATION

### Corresponding Author

\*E-mail: [kris.ooms@kingsu.ca](mailto:kris.ooms@kingsu.ca).

## Notes

The authors declare no competing financial interest.

## ■ ACKNOWLEDGMENTS

The authors thank the members of the Faculty of Natural Sciences at The King's University College for helpful comments. The Natural Sciences and Engineering Research Council of Canada and King's are thanked for financial support.

## ■ REFERENCES

- (1) Momirlan, M.; Veziroglu, T. N. *Int. J. Hydrogen Energ.* **2005**, *30*, 795–802.
- (2) Zhang, H.; Shen, P. K. *Chem. Rev.* **2012**, *112*, 2780–2832.
- (3) Brunello, G.; Lee, S. G.; Jang, S. S.; Qi, Y. *J. Renew. Sustain. Energy* **2009**, *1*, 033101/1–033101/14.
- (4) Kreuer, K. D. *J. Membr. Sci.* **2001**, *185*, 29–39.
- (5) Mahajan, C. V.; Ganesan, V. *J. Phys. Chem. B* **2010**, *114*, 8367–8373.
- (6) Mahajan, C. V.; Ganesan, V. *J. Phys. Chem. B* **2010**, *114*, 8357–8366.
- (7) Krivobokov, I. M.; Gribov, E. N.; Okunev, A. G. *Electrochim. Acta* **2011**, *56*, 2420–2427.
- (8) Kaliaguine, S.; Mikhailenko, S. D.; Wang, K. P.; Xing, P.; Robertson, G.; Guiver, M. *Catal. Today* **2003**, *82*, 213–222.
- (9) Li, N.; Shin, D. W.; Hwang, D. S.; Lee, Y. M.; Guiver, M. D. *Macromolecules* **2010**, *43*, 9810–9820.
- (10) Fathima, N. N.; Aravindhan, R.; Lawrence, D.; Yugandhar, U.; Moorthy, T. S. R.; Nair, B. U. *J. Sci. Ind. Res.* **2007**, *66*, 209–219.
- (11) Li, X.; Zhang, G.; Xu, D.; Zhao, C.; Na, H. *J. Power Sources* **2007**, *165*, 701–707.
- (12) Alberti, G.; Narducci, R.; Sganappa, M. *J. Power Sources* **2008**, *178*, 575–583.
- (13) Gebel, G. *Polymer* **2000**, *41*, 5829–5838.
- (14) Ye, G.; Janzen, N.; Goward, G. R. *Macromolecules* **2006**, *39*, 3283–3290.
- (15) Kreuer, K. D. *Solid State Ionics* **1997**, *97*, 1–15.
- (16) Perrin, J. C.; Lyonard, S.; Volino, F. *J. Phys. Chem. C* **2007**, *111*, 3393–3404.
- (17) Cui, S.; Liu, J.; Selvan, M. E.; Keffer, D. J.; Edwards, B. J.; Steele, W. V. *J. Phys. Chem. B* **2007**, *111*, 2208–2218.
- (18) Jang, S. S.; Molinero, V.; Cagin, T.; Goddard, W. A., III. *J. Phys. Chem. B* **2004**, *108*, 3149–3157.
- (19) Huang, R. Y. M.; Shao, P.; Burns, C. M.; Feng, X. *J. Appl. Polym. Sci.* **2001**, *82*, 2651–2660.
- (20) Paik, Y.; Chae, S. A.; Han, O. H.; Hwang, S. Y.; Ha, H. Y. *Polymer* **2009**, *50*, 2664–2673.
- (21) Keinan-Adamsky, K.; Shinar, H.; Navon, G. *J. Orthop. Res.* **2005**, *23*, 109–117.
- (22) Keinan-Adamsky, K.; Shinar, H.; Navon, G. *Magn. Reson. Mater. Phys.* **2005**, *18*, 231–237.
- (23) Sharf, Y.; Akselrod, S.; Navon, G. *Magn. Reson. Med.* **1997**, *37*, 69–75.
- (24) Sharf, Y.; Seo, Y.; Eliav, U.; Akselrod, S.; Navon, G. *Proc. Natl. Acad. Sci. U.S.A.* **1998**, *95*, 4108–4112.
- (25) Shinar, H.; Seo, Y.; Ikoma, K.; Kusaka, Y.; Eliav, U.; Navon, G. *Magn. Reson. Med.* **2002**, *48*, 322–330.
- (26) Shinar, H.; Seo, Y.; Navon, G. *Rev. Neurosci.* **2005**, *16*, S59–S59.
- (27) Vanderveen, J. R.; Blackburn, M. A.; Ooms, K. J. *Can. J. Chem.* **2011**, *89*, 1095–1104.
- (28) Perea, W.; Cannella, M.; Yang, J.; Vega, A. J.; Polenova, T.; Marcolongo, M. *Magn. Reson. Med.* **2007**, *57*, 990–999.
- (29) Sun, C.; Boutis, G. S. *J. Magn. Reson.* **2010**, *205*, 86–92.
- (30) Li, J.; Wilmsmeyer, K. G.; Madsen, L. A. *Macromolecules* **2008**, *41*, 4555–4557.
- (31) Li, J.; Wilmsmeyer, K. G.; Madsen, L. A. *Macromolecules* **2009**, *42*, 255–262.
- (32) Hou, J.; Li, J.; Madsen, L. A. *Macromolecules* **2010**, *43*, 347–353.
- (33) Xu, G.; Pak, Y. S. *Solid State Ionics* **1992**, *50*, 339–43.
- (34) Rankothge, M.; Haryadi; Moran, G.; Hook, J.; Van Gorkom, L. *Solid State Ionics* **1994**, *67*, 241–8.
- (35) Sharf, Y.; Eliav, U.; Shinar, H.; Navon, G. *J. Magn. Reson. B* **1995**, *107*, 60–67.
- (36) Devanathan, R.; Venkatnathan, A.; Dupuis, M. *J. Phys. Chem. B* **2007**, *111*, 8069–8079.
- (37) Halle, B. *Magn. Reson. Med.* **2006**, *56*, 60–72.
- (38) Abragam, A. In *Principles of nuclear magnetism*; Oxford University Press: Oxford, 1962.